Accuracy of density functional theory methods for the calculation of magnetic exchange couplings in binuclear iron(III) complexes

Rajendra P. Joshi [a], Jordan J. Phillips [a], Kylie J. Mitchell [b], George Christou [b], Koblar A. Jackson [a], Juan E. Peralta [a,*]

[a] Department of Physics and Science of Advanced Materials, Central Michigan University, Mount Pleasant, MI 48859, USA
[b] Department of Chemistry, University of Florida, Gainesville, Florida 32611-7200, United States

ARTICLE INFO

ABSTRACT

We assess the performance of popular hybrid density functional approximations for the prediction of magnetic exchange couplings (J) in Fe^{III} complexes. To this end, eleven dinuclear oxo-bridged iron(III) complexes with accurately determined J values were chosen to cover cases of weak and strong antiferromagnetic couplings ranging from $-6 \, cm^{-1}$ to $-132 \, cm^{-1}$. Seven representative exchange-correlation functionals ranging from the hybrids PBEh and B3LYP to meta hybrids (M06, M062X), range separated functionals (HSE, LC-ωPBE), and LSDA with 30% of HF exchange were used for this assessment. These functionals have been suggested as good performers for this particular property in transition metal complexes and hence this assessment aims to narrow the interval of confidence for the particular case of Fe complexes. In addition, we examined the performance of an alternative method based on differential local spin rotations to calculate magnetic exchange coupling parameters in these complexes. Our results show that, although some of these functionals perform on par, the M06 and HSE functionals yield magnetic exchange couplings in closer agreement with experimental data, with mean absolute percentage errors of 8.6 and 9.2%, respectively.

© 2019 Elsevier Ltd. All rights reserved.

1. Introduction

Transition metal (TM) complexes show distinct magnetic properties due to the presence of exchange interactions between metal centers [1,2], spin-orbit coupling [3], and their variable coordination number [4] and oxidation state. Their characteristic low dimensionality and their capability to exhibit different spin ground states as a result of competing magnetic interactions make these complexes of significant interest as potential molecular magnets (MM) [5], spintronics devices [6], memory chips [7], and quantum computing units [8]. Moreover, they are widely studied by biochemists due to their crucial role in several biochemical processes [9].

Theoretical and experimental studies of the magnetic properties of transition metal complexes have been directed towards designing novel molecular magnets with desired properties and performance [5,10–12,13–17]. Many of these studies employ magneto-structural correlations to predict and understand the origin of the magnetic interactions. This has been accomplished

experimentally by magnetochemical studies, while from the theoretical side, several electronic structure methods have been employed, broadly divided into wave function-based post-Hartree-Fock [18–21], and Kohn-Sham (KS) density functional theory (DFT) [22] methods. While the former provide a systematically improvable and generally accurate route to calculating magnetic properties, calculations on medium- and large-size TM complexes using these methods are unaffordable. DFT methods, on the other hand, provide a widely-used and computationally accessible alternative to wave function methods that have found routine use as a tool for the prediction of electronic properties of materials ranging from molecules to solids. Despite the fact that DFT is an exact theory in principle, in practice the choice of the approximate exchange correlation energy functional (E_{XC}) [23] determines the accuracy of the calculations. The practical realization of DFT started with the development of local density approximation (LDA) [24,25] where E_{XC} only depends upon the local electron density. The LDA [25] performs reasonably well for some systems and properties but fails for many others. The generalized gradient approximation (GGA) [26,27] was introduced by incorporating gradients of the electron density, and although it improves upon the LDA in several respects, it still falls short for properties such as dissociation energies,

---

* Corresponding author.
E-mail address: peral1j@cmich.edu (J.E. Peralta).

energy gaps, and magnetic properties [26]. Magnetic exchange couplings calculated with LDA and GGA in diverse TM complexes are on average 6 to 11 times larger than reference experimental values [28].

With the advent of hybrid functionals, DFT has gained more accuracy for several molecular properties and reached a larger variety of systems. These functionals are widely implemented in DFT codes and their accuracy for the prediction of structural and electronic properties of materials is well documented [29–31,28]. Although the performance of hybrid density functionals for magnetic exchange couplings has been analyzed in the past, deviations from accurate experimental data are typically larger than for other properties [32–34]. With the significant advances in the quality of density functionals in the past years, there is always interest regarding their reliability for the calculation of magnetic properties [35,27,36–38,29,39–41,31,42,43,30,44,45]. For instance, Phillips et al. [28] have shown statistical errors of about 40% in a set of 14 bimetallic homonuclear transition metal complexes containing Fe, Mn, Cu, V metals. Since the interactions that take place in these complexes are very different (giving a range of exchange couplings from -382 cm^{-1} to $+114$ cm^{-1}), it is reasonable to wonder what is the performance of hybrid density functionals in a set of same-metal homonuclear TM complexes. This type of analysis can provide a more focused appraisal of practical use. In this work, we assess the performance of representative density functionals for the prediction of magnetic exchange couplings involving Fe^{III} centers. This has two goals: to assess the performance of these functionals and also to determine the expected errors for this specific type of exchange couplings. To this end, we selected a set of 11 dinuclear oxo-bridged Fe^{III} complexes with accurately determined experimental J couplings. These complexes were chosen so that they can be considered as representative of typical oxo-bridged Fe^{III}–Fe^{III} moieties and hence the conclusions can be extrapolated to larger Fe^{III} complexes. It should be mentioned that this assessment validates the ability of the selected DFT approximations to reproduce J couplings, and not the errors in the resulting densities associated with these functionals [46], which could affect other magnetic properties.

2. Computational details

For most TM complexes, magnetic interactions are typically modeled using the Heisenberg-Dirac-van-Vleck Hamiltonian [47] in terms of the magnetic exchange coupling parameter J_{ab} defined by

$$H_{HDVV} = -2\sum_{a<b} J_{ab} \vec{S}_a \cdot \vec{S}_b, \tag{1}$$

where S_a and S_b are the (localized) spin moments on magnetic centers a and b, respectively. For a dinuclear system, J_{ab} can be extracted from DFT calculations using high-spin (HS) and broken symmetry (BS) DFT reference states using

$$J_{ab} = \frac{E_{BS} - E_{HS}}{4S_a S_b}. \tag{2}$$

This approach is referred to as BS-DFT and its accuracy depends on the choice of the approximate E_{XC} employed [48,49].

In addition, in this work we have investigated the performance of a recently proposed method for calculating magnetic exchange coupling parameters starting from a particular spin configuration, either HS or BS. This method is based on a generalized perturbative approach within DFT where magnetic exchange coupling parameters are given by the analytic second derivative of the energy with respect to local spin rotations.

$$J = \frac{1}{2S_1 S_2} \frac{d^2}{d\theta^2} \left\langle \widehat{H}_{HDVV} \right\rangle \bigg|_{\theta=0}. \tag{3}$$

Within this method, the relative angle between two spins is used as a constraint, while a torque on the local spin is used as a small perturbation. We refer readers to Refs. [50,51] for details. Other related methods for the calculation of exchange couplings in molecules that utilize approximate differential local spin rotations based on Green's functions have been proposed [52,53]. Within this approach, the explicit determination of different spin solutions is avoided and, instead, the noncollinear coupled-perturbed KS equations need to be solved to determine the second derivative in Eq. (3). We refer to this method as BB for black-box. One of the drawbacks of the BB method is its difficulty to converge self-consistently when using a density functional that includes a GGA component. For this reason we have adopted the local LSDA exchange-correlation functional with 30% of HF exchange in it (herein called LSDA30) for all calculations using this method.

Fig. 1 shows the molecular complexes used in this work. These complexes have been investigated by single-crystal X-ray diffractometry and magnetochemical studies. Structural parameters for the complexes were taken from the corresponding crystal structures. All the complexes considered here are dinuclear Fe$_2^{III}$, and most have a single bridging oxido (O^{2-}) ion with either zero, one, or two additional bridging ligands to provide a variety of structural types, bridging Fe-O bond lengths and Fe-O-Fe angles, and resulting relatively strong exchange couplings (complexes 1-7). In addition, we include four complexes that are doubly-bridged either by two methoxo (MeO$^-$) ions (complexes 10 and 11), or alkoxo- or phenoxo-units within more complicated bridging ligands (complexes 8 and 9, respectively). These latter four complexes are known experimentally to exhibit much weaker exchange couplings than oxido-bridged complexes, ensuring a wide range of coupling strengths for our computational study. In all of these complexes, the Fe atoms are in a +3 oxidation state with five unpaired electrons in 3d orbitals, and the magnetization originates mainly due to the interaction between magnetic moments at the metal centers with negligible contribution from other atoms in the ligands attached to them. For consistency, all J coupling calculations in this work were carried out using each experimentally determined crystal structure. All complexes considered have experimental antiferromagnetic exchange coupling parameters ranging from -6 cm^{-1} to -132 cm^{-1}, and all the HS states have an effective spin multiplicity of 11 while the BS states have a multiplicity of 1.

For all calculations we have used the Gaussian09 suite of programs [54] to evaluate the total energy for the HS and BS spin states with seven exchange correlation functionals, starting from the local hybrid LSDA30 to the widely used hybrid functionals PBEh [27,36,37] and B3LYP [26,55,35,56,57], to the meta hybrid functionals M06, M062X [30], and finally range separated functionals HSE [38,29,39–41] and LC-ωPBE [31,42,43]. LSDA30 is the hybrid of LSDA with 30% HF exchange which has been previously described. PBEh [28,36,37] is the hybrid functional of Perdew, Burke and Ernezerhnof (also known as PBE0 or PBE1PBE in the literature) with 75% of its exchange energy determined by PBE exchange and 25% from Hartree-Fock exchange, with correlation from the PBE functional. The meta-GGA functionals M06 and M062X admix 27% and 54% HF exchange, respectively, with DFT exchange [30]. We employed the 2006 version of the hybrid HSE [38] (also known as HSE06 in the literature; keyword `HSEH1PBE` in Gaussian), which admixes short-range screened Hartree-Fock exchange in the functional realization. LC-ωPBE [58] is a long-range corrected GGA functional which partitions exchange interactions into short and long range terms where short range-exchange interactions are described with PBE exchange while long range
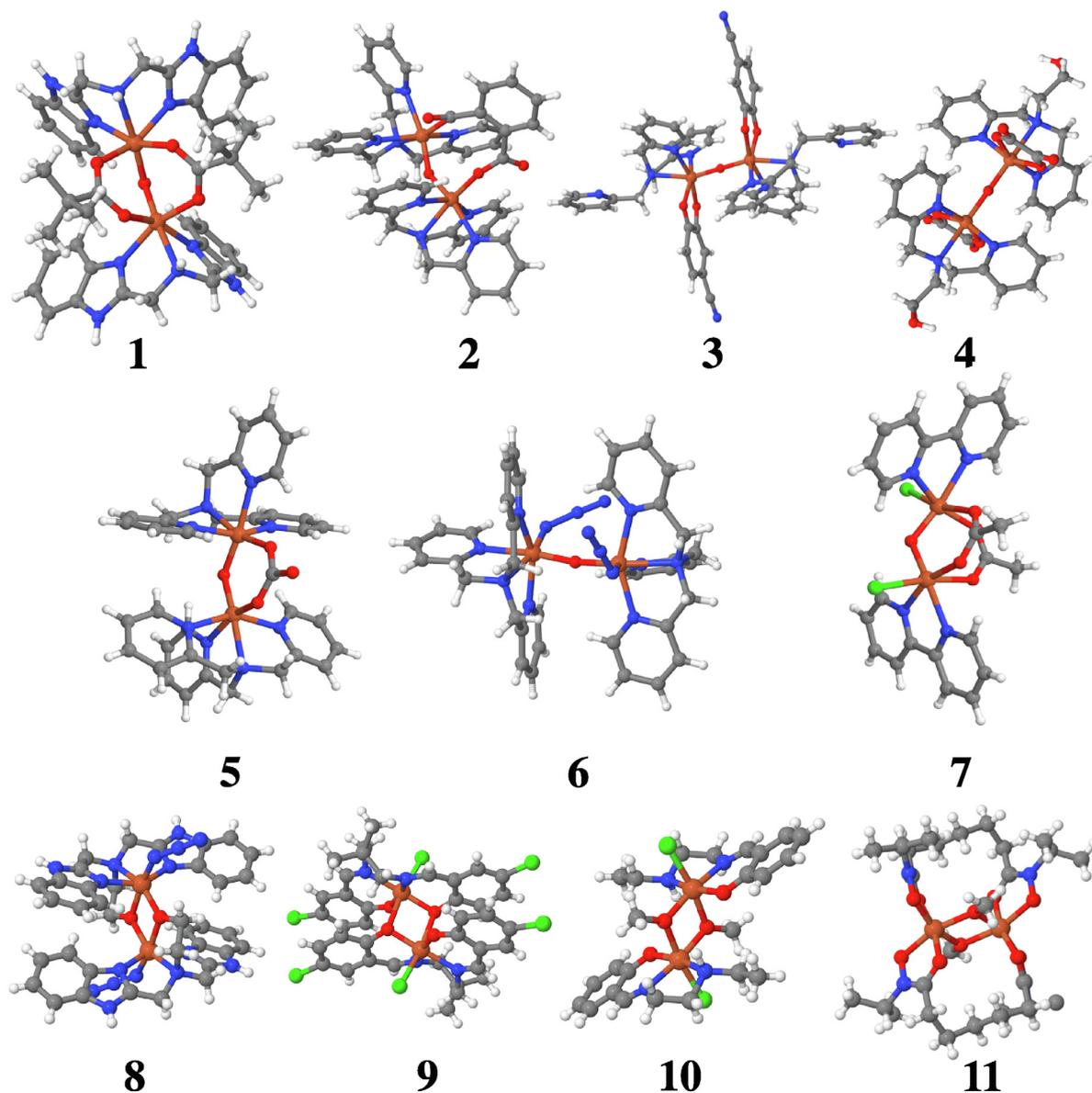
Fig. 1. Crystal structures of the complexes considered in this work with their CCDC names (**1**) JEJVEZ, (**2**) VIGHEY, (**3**) FAJPUD, (**4**) FAJQEO, (**5**) VIGGUN, (**6**) FAJQAK, (**7**) VABMUG, (**8**) ABIZOA, (**9**) ELISAU, (**10**) BAZCOV, (**11**) BOSMOL10. Here, the Fe are represented by dark brown balls, oxygen by red, nitrogen by blue, chlorine by green, carbon by gray, and hydrogen by white. (For interpretation of the references to colour in this figure legend, the reader is referred to the web version of this article.)

interactions are treated by HF exchange. Convergence to the target magnetic state was confirmed by a minimum basis set (MBS) Mulliken spin population analysis [59]. All calculations were converged to 10^{-6} ha = 0.2 cm^{-1} in energy and 10^{-8} RMS change in the density matrix.

3. Results and discussion

We first checked for a suitable basis set for our calculations by examining the basis set dependence of J for the particular complex **2** as a representative case with the choice of M06 exchange-correlation functional. Five different basis set were employed for this purpose: (i) 6-31G** on all atoms, (ii) 6-311G** on all atoms, (iii) 6-311+G* on all atoms, (iv) 6-311+G** on all atoms, and (v) 6-311+G** for Fe and 6-31G** for C, N, O, H atoms. The calculated J couplings for these basis sets are -106.7, -111.0, -109.0, -109.0, and -109.6 cm^{-1} for the basis set (i), (ii), (iii), (iv), and

(v), respectively. These results show that although all these basis sets give comparable J couplings, option (v) provides a reasonable compromise between quality and computational effort. All further calculations in this work were performed with this choice of basis set.

In Table 1 we show the calculated exchange couplings for all the complexes using the different exchange-correlation functionals along with the experimentally determined couplings. For all the complexes, HSE and PBEh give fairly similar results, with HSE being slightly closer to experimental values compared to the PBEh couplings. Although LC-ωPBE performs very well in a number of applications such as energy barriers, bond lengths, thermochemistry, and long-range charge transfer process for molecular systems [31], our results show that this long-range corrected hybrid functional generally overestimates Fe–Fe J couplings. On the other hand, J couplings calculated with the meta GGA hybrid functional M06, which admixes 27% of Hartree Fock exchange, are in good agreement with experiments. This contrasts with our early

Table 1
Magnetic exchange couplings (cm^{-1}) for the dinuclear iron complexes considered in this work using the BS approach. For the LSDA30, couplings using both the BS approach and the BB method are shown.

| Complex | Functional | | | | | | | | |
| | HSE | PBEh | B3LYP | LC-ωPBE | M06 | M062X | LSDA30 | | Exp. |
							BS	BB	
1	−112.6	−109.8	−132.2	−121.5	−116.9	−68.3	−99.4	−106.6	−116.0[a]
2	−112.0	−106.5	−124.9	−119.4	−109.6	−69.1	−96.8	−106.0	−110.0[b]
3	−95.4	−95.0	−106.2	−112.9	−94.5	−67.9	−86.3	−95.4	−78.0[c]
4	−97.1	−95.7	−109.9	−115.4	−97.6	−64.5	−86.8	−93.1	−98.0[c]
5	−100.0	−98.0	−110.2	−102.7	−103.9	−59.6	−84.8	−94.4	−108.0[b]
6	−103.6	−102.0	−117.1	−117.6	−104.3	−69.8	−93.0	−99.9	−90.0[c]
7	−113.6	−111.1	−132.3	−124.8	−116.4	−70.3	−100.3	−111.0	−132.0[d]
8	−18.7	−18.6	−22.2	−20.3	−20.3	−9.8	−16.3	−15.5	−21.3[e]
9	−5.9	−5.8	−7.6	−4.9	−6.7	−3.2	−4.9	−4.5	−6.4[f]
10	−15.0	−14.8	−18.2	−14.9	−15.4	−7.2	−12.3	−11.6	−13.65[g]
11	−11.0	−10.9	−13.3	−11.8	−12.0	−5.2	−8.6	−7.8	−10.9[h]

[a] Taken from Ref. [65].
[b] Taken from Ref. [66].
[c] Taken from Ref. [67].
[d] Taken from Ref. [68].
[e] Taken from Ref. [69].
[f] Taken from Ref. [70].
[g] Taken from Ref. [71].
[h] Taken from Ref. [72].

findings for a set of 6 heterodinuclear TM complexes where HSE performs much better than M06 [51]. Our results with the M062X functional (containing 54% of Hartree Fock exchange) show that in this case, increasing the Hartree Fock exchange admixture beyond a certain limit has an adverse effect on the value of the exchange coupling parameter, leading to a severe underestimation of the strength of the antiferromagnetic interaction.

It should be mentioned that another popular alternative to the BS-DFT approach for mapping DFT energies into J couplings is based on Yahagughi's formula, which effectively replaces $4S_aS_b$ by $\left\langle S^2 \right\rangle_{HS} - \left\langle S^2 \right\rangle_{BS}$ in Eq. (2) [60,61]. For our calculations, $S_a = S_b = 5/2$, and $\left\langle S^2 \right\rangle_{HS} \approx 30$ and $\left\langle S^2 \right\rangle_{BS} \approx 5$ in all cases due to the large localization of the spins at the Fe centers, which makes both approaches yield very similar values, typically within 1%.

We show in Table 1 J couplings calculated with LSDA30 using both the energy-differences BS-DFT approach and the BB method. For this particular functional, calculated J couplings using the BS-DFT approach are systematically underestimated (in absolute value) when compared to their BB counterparts. This can be understood intuitively, recalling that J couplings obtained with the BB approach are formally identical to the energy-differences couplings only in the case of an ideal (perfectly localized) HDVV system, where the curvature of the energy as a function of the inter-spin angle is perfectly quadratic [50]. In real complexes, a small deviation of the BB couplings (calculated at the HS or BS states) from the BS-DFT results can be expected. Our results show that in this particular case, the choice of the methodology could have an effect comparable to the choice of the XC functional. However, the advantage of the BB method is highlighted in the case of large multicenter systems, where it requires only one spin state to calculate J, and hence it is free from typical problems arising from the BS-DFT approach, such as convergence difficulties for some BS solutions or convergence to undesired solutions.

For all the calculations performed in this work, the slight deviation between the experimental and theoretical values may be also partly attributed, among other reasons, to the fact that calculations are performed in gas phase and zero K, in contrast to experimental crystal phase and temperature dependent experiments. In this regard, our assessment gives an estimation of the errors originating

in the entire protocol for evaluating exchange couplings, and not only in the exchange-correlation functional chosen. The absolute percentage error of calculated J couplings with respect to experiments is shown as a bar plot in Fig. 2.

We have identified a few weakly ferromagnetically-coupled dinuclear azido-bridged Fe_2^{III} complexes in the CCDC database [62–64] with J couplings between +0.8 and +2.4 cm^{-1}. For the complex with the largest ferromagnetic coupling (CCSD name RIJLAX; Ref. [62]) we found that the calculated J is ferromagnetic, with
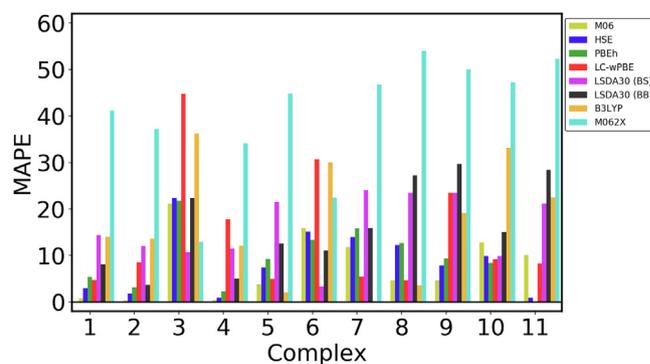
Fig. 2. Absolute percentage error of the calculated J couplings with respect to the experimental results for each complex.

Table 2
Standard error deviation (in cm^{-1}), mean percentage error (MPE), and mean absolute percentage error (MAPE) for different exchange-correlation functionals.

Method	Standard error deviation	MPE	MAPE
HSE	9.6	0.8	9.2
PBEh	10.1	−0.9	9.6
B3LYP	10.5	17.2	17.2
LC-ωPBE	13.7	8.1	15.8
M06	8.5	4.4	8.6
M062X	20.8	−40.2	40.2
LSDA30 (BS)	11.9	−13.3	16.1
LSDA30 (BB)	10.4	−10.4	17.1

Table 3
Minimum basis set Mulliken (MBS) atomic spin populations for the high spin (HS) and broken symmetry (BS) states for different dinuclear iron complexes and density functional approximations.

Complex	Functional									
	HSE		PBEh		LC-ωPBE		M06		M062X	
	HS	BS	HS	BS	HS	BS	HS	BS	HS	BS
1	4.40	−4.37	4.41	−4.38	4.42	−4.38	4.41	−4.38	4.52	−4.51
2	4.39	−4.34	4.40	−4.35	4.41	−4.35	4.40	−4.35	4.52	−4.49
3	4.36	−4.32	4.37	−4.32	4.39	−4.33	4.38	−4.32	4.50	−4.47
4	4.38	−4.33	4.39	−4.34	4.41	−4.35	4.38	−4.33	4.51	−4.48
5	4.36	−4.34	4.37	−4.34	4.39	−4.35	4.36	−4.33	4.49	−4.44
6	4.35	−4.29	4.36	−4.29	4.36	−4.30	4.34	−4.29	4.48	−4.45
7	4.37	−4.34	4.37	−4.34	4.39	−4.35	4.37	−4.34	4.49	−4.48
8	4.34	−4.34	4.34	−4.34	4.36	−4.36	4.34	−4.34	4.50	−4.50
9	4.37	−4.37	4.37	−4.37	4.39	−4.39	4.37	−4.37	4.51	−4.51
10	4.38	−4.38	4.37	−4.37	4.39	−4.39	4.37	−4.37	4.52	−4.52
11	4.41	−4.41	4.41	−4.41	4.43	−4.43	4.41	−4.41	4.54	−4.54

values of about 6 cm^{-1} for B3LYP and PBEh. This indicates that, even though these complexes fall outside the oxo-bridged category, this same protocol for evaluating exchange couplings can also predict ferromagnetic couplings.

We have also evaluated the standard deviation, mean percentage error and mean absolute percentage error in the calculated exchange couplings for each functional and show it in Table 2. Our results indicate that the M06 functional (with a standard error deviation and mean absolute percentage error of 8.5 cm^{-1} and 8.6%, respectively) is the most accurate functional for the calculation of Fe-Fe exchange couplings, compared to the other functionals considered, followed closely by HSE and PBEh, while M062X gives the largest error. The LSDA30 functional in combination with the BS energy-differences approach shows a relatively large standard deviation and mean absolute error, while this same functional performs slightly better when used with our BB method. This can be likely attributed to a compensation of factors: on the one hand, the LSDA30 tends to underestimate the coupling in absolute value (Table 1), while the second derivative of the energy with respect to local spin rotations given by the BB method is slightly larger than that of an ideal HDVV system.

We analyzed the atomic spin population dependence of each HS and BS state on the choice of exchange-correlation functionals using the minimum basis set Mulliken (MBS) population analysis. Our calculations show a small deviation from the nominal spin values of 5.0 at the Fe^{III} centers, as shown in Table 3 for some selected functionals. This is expected as a result of a delocalization of the unpaired 3d electrons to the ligands. We obtained MBS spin populations at the Fe centers between 4.3 and 4.5 (in absolute value) in all cases, with larger values corresponding to M062X, which can be attributed to the increased localization produced by larger HFX contribution (54%) compared with other functionals in this work [73]. This larger localization can be related to the poor performance of M062X for this particlar case.

4. Conclusions

In this work we assessed the performance of seven popular hybrid density functional approximations for the calculation of Fe-Fe magnetic exchange coupling constants by comparing with reliable experimental values. Using the broken-symmetry energy-differences approach, our results show that the M06 exchange-correlation functional can predict Fe–Fe J couplings with a mean absolute percentage error (MAPE) of 8.6%, while HSE and PBEh yield slightly larger, but still small, MAPEs of 9.2% and 9.6%, respectively. We have also included in our assessment the BB method in combination with the hybrid LSDA30 functional and

show that in this case we get as similar MAPE as can be expected. Our analysis provides an estimate of the error in the prediction of magnetic exchange coupling constants in the density functional theory framework, particularly hybrid functionals, for the case of oxo-bridged Fe^{III} complexes.

Hybrid functionals differ from the corresponding non-hybrids by including some fraction of exact exchange in the description of the electron-electron interaction. One result of this is to lessen the magnitude of one-electron self-interaction error (SIE) that arises from approximating the exact exchange-correlation functional. SIE can have a substantial impact on the performance of a non-hybrid functional. In recent work [74], some of us demonstrated that removing self-interaction effects from LSDA directly, by applying the Fermi-Löwdin orbital self-interaction correction (FLO-SIC), significantly improves the description of magnetic exchange couplings in a set of organic biradicals and in a Cu-based bimetallic complex. Removing self-interaction results in greater localization of unpaired electrons. This correctly increases the size of the calculated couplings for the radicals, while shrinking it for the bimetallic complex. The FLO-SIC-LDA results are competitive with PBEh results overall, and better in many cases. How FLO-SIC would perform for high-spin systems like the Fe^{III} complexes described in this paper is an open question that we are currently addressing. The present results offer useful data for any electronic structure method.

References

[1] S. Hill, R.S. Edwards, N. Aliaga-Alcalde, G. Christou, Quantum coherence in an exchange-coupled dimer of single-molecule magnets, Science 302 (5647) (2003) 1015–1018, https://doi.org/10.1126/science.1090082.

[2] Y. Ida, S. Ghosh, A. Ghosh, H. Nojiri, T. Ishida, Strong ferromagnetic exchange interactions in hinge-like dy(o2cu)2 complexes involving double oxygen bridges, Inorg. Chem. 54 (19) (2015) 9543–9555, https://doi.org/10.1021/acs.inorgchem.5b01583.

[3] J.B. Goodenough, Spin-orbit-coupling effects in transition-metal compounds, Phys. Rev. 171 (1968) 466–479, https://doi.org/10.1103/PhysRev.171.466.

[4] C.A. Blindauer, M.T. Razi, S. Parsons, P.J. Sadler, Metal complexes of n,n,n-,n-tetrakis(2-pyridylmethyl)ethylenediamine (tpen): variable coordination numbers and geometries, Polyhedron 25 (2) (2006) 513–520, https://doi.org/10.1016/j.poly.2005.08.019, special issue in honour of Malcolm H. Chisholm.

[5] A.V. Postnikov, J. Kortus, M.R. Pederson, Density functional studies of molecular magnets, Phys. Status Solidi B 243 (11) (2006) 2533–2572, https://doi.org/10.1002/pssb.200541490.

[6] H.B. Heersche, Z. de Groot, J.A. Folk, H.S.J. van der Zant, C. Romeike, M.R. Wegewijs, L. Zobbi, D. Barreca, E. Tondello, A. Cornia, Electron transport through single Mn_{12} molecular magnets, Phys. Rev. Lett. 96 (2006), https://doi.org/10.1103/PhysRevLett.96.206801 206801.

[7] H. Fukunaga, H. Miyasaka, Magnet design by integration of layer and chain magnetic systems in a π-stacked pillared layer framework, Angew. Chem. Int. Edit. 54 (2) (2014) 569–573, https://doi.org/10.1002/anie.201410057.

[8] D. Stepanenko, M. Trif, D. Loss, Quantum computing with molecular magnets, Inorg. Chim. Acta 361 (14-15) (2008) 3740–3745, https://doi.org/10.1016/j.ica.2008.02.066.

[9] B. Kok, B. Forbush, M. Mcgloin, Cooperation of charges in photosynthetic O_2 evolution. A linear four step mechanism, Photochem. Photobio. 11 (6) (1970) 457–475, https://doi.org/10.1111/j.1751-1097.1970.tb06017.x.

[10] W. Wernsdorfer, N. Aliaga-Alcalde, D.N. Hendrickson, G. Christou, Exchange-biased quantum tunnelling in a supramolecular dimer of single-molecule magnets, Nature 416 (2002) 406–409, https://doi.org/10.1038/416406a.

[11] R. Bagai, W. Wernsdorfer, K.A. Abboud, G. Christou, Exchange-biased dimers of single-molecule magnets in off and on states, J. Am. Chem. Soc. 129 (43) (2007) 12918–12919, https://doi.org/10.1021/ja075382o.

[12] L. Bogani, W. Wernsdorfer, Molecular spintronics using single-molecule magnets, Nat. Mater. 7 (2008) 179, https://doi.org/10.1038/nmat2133.

[13] J.J. Phillips, J.E. Peralta, G. Christou, Magnetic couplings in spin frustrated Fe_7^{III} disklike clusters, J. Chem. Theory Comput. 9 (12) (2013) 5585–5589, https://doi.org/10.1021/ct4007376.

[14] J.I. Melo, J.J. Phillips, J.E. Peralta, Structural dependence of magnetic exchange coupling parameters in transition-metal complexes, Chem. Phys. Lett. 557 (2013) 110–113, https://doi.org/10.1016/j.cplett.2012.12.013.

[15] J.E. Peralta, O. Hod, G.E. Scuseria, Magnetization dynamics from time-dependent noncollinear spin density functional theory calculations, J. Chem. Theory and Comput. 11 (8) (2015) 3661–3668, https://doi.org/10.1021/acs.jctc.5b00494.

[16] A. Rodrguez-Fortea, E. Ruiz, P. Alemany, S. Alvarez, Magneto-structural correlations in trinuclear Cu(II) complexes: A density functional study, Monatshefte für Chemie / Chemical Monthly 134 (2) (2003) 307–316, https://doi.org/10.1007/s00706-002-0523-6.

[17] E.A. Suturina, D. Maganas, E. Bill, M. Atanasov, F. Neese, Magneto-structural correlations in a series of pseudotetrahedral $[CoII(Xr)_4]^{2-}$ single molecule magnets: an ab initio ligand field study, Inorg. Chem. 54 (20) (2015) 9948–9961, https://doi.org/10.1021/acs.inorgchem.5b01706.

[18] K. Andersson, P. Malmqvist, B.O. Roos, Second-order perturbation theory with a complete active space self-consistent field reference function, J. Chem. Phys. 96 (2) (1992) 1218–1226, https://doi.org/10.1063/1.462209.

[19] K. Andersson, P.A. Malmqvist, B.O. Roos, A.J. Sadlej, K. Wolinski, Second-order perturbation theory with a CASSCF reference function, J. Phys. Chem. 94 (14) (1990) 5483–5488, https://doi.org/10.1021/j100377a012.

[20] V. Garca, O. Castell, R. Caballol, J. Malrieu, An iterative difference-dedicated configuration interaction. proposal and test studies, Chem. Phys. Lett. 238 (4–6) (1995) 222–229, https://doi.org/10.1016/0009-2614(95)00438-A.

[21] O. Castell, V.M. García, C. Bo, R. Caballol, Relative stability of the 3a2, 1a2, and 1a1 states of phenylnitrene: a difference-dedicated configuration interaction calculation, J. Comput. Chem. 17 (1) (1996) 42–48, https://doi.org/10.1002/(SICI)1096-987X(19960115)17:1<42::AID-JCC4>3.0.CO;2-0.

[22] P. Hohenberg, W. Kohn, Inhomogeneous electron gas, Phys. Rev. 136 (1964) B864–B871, https://doi.org/10.1103/PhysRev.136.B864.

[23] A.K. Rajagopal, J. Callaway, Inhomogeneous electron gas, Phys. Rev. B 7 (1973) 1912–1919, https://doi.org/10.1103/PhysRevB.7.1912.

[24] W. Kohn, L.J. Sham, Self-consistent equations including exchange and correlation effects, Phys. Rev. 140 (1965) A1133–A1138, https://doi.org/10.1103/PhysRev.140.A1133.

[25] U. von Barth, L. Hedin, A local exchange-correlation potential for the spin polarized case I, J. Phys. C: Solid State Phys. 5 (13) (1972) 1629.

[26] A.D. Becke, Density-functional exchange-energy approximation with correct asymptotic behavior, Phys. Rev. A 38 (1988) 3098–3100, https://doi.org/10.1103/PhysRevA.38.3098.

[27] J.P. Perdew, K. Burke, M. Ernzerhof, Generalized gradient approximation made simple, Phys. Rev. Lett. 77 (1996) 3865–3868, https://doi.org/10.1103/PhysRevLett.77.3865.

[28] J.J. Phillips, J.E. Peralta, Magnetic exchange couplings from semilocal functionals evaluated nonself-consistently on hybrid densities: insights on relative importance of exchange, correlation, and delocalization, J. Chem. Theory Comput. 8 (9) (2012) 3147–3158, https://doi.org/10.1021/ct3004904.

[29] J. Heyd, G.E. Scuseria, Efficient hybrid density functional calculations in solids: assessment of the heyd-scuseria-ernzerhof screened coulomb hybrid functional, J. Chem. Phys. 121 (3) (2004) 1187–1192, https://doi.org/10.1063/1.1760074.

[30] Y. Zhao, D. Truhlar, The M06 suite of density functionals for main group thermochemistry, thermochemical kinetics, noncovalent interactions, excited states, and transition elements: two new functionals and systematic testing of four M06-class functionals and 12 other functionals, Theor. Chem. Acc. 120 (1–3) (2008) 215–241, https://doi.org/10.1007/s00214-007-0310-x.

[31] O.A. Vydrov, G.E. Scuseria, Assessment of a long-range corrected hybrid functional, J. Chem. Phys. 125 (23) https://doi.org/10.1063/1.2409292.

[32] P. Rivero, I. d P.R. Moreira, F. Illas, G.E. Scuseria, Reliability of range-separated hybrid functionals for describing magnetic coupling in molecular systems, J. Chem. Phys. 129 (18) (2008) 184110, https://doi.org/10.1063/1.3006419.

[33] E. Ruiz, Exchange coupling constants using density functional theory: long-range corrected functionals, J. Comp. Chem. 32 (9) (2011) 1998–2004, https://doi.org/10.1002/jcc.21788.

[34] E. Ruiz, S. Alvarez, J. Cano, V. Polo, About the calculation of exchange coupling constants using density-functional theory: the role of the self-interaction error, J. Chem. Phys. 123 (16) (2005), https://doi.org/10.1063/1.2085171 164110.

[35] A.D. Becke, Density-functional thermochemistry. III. The role of exact exchange, J. Chem. Phys. 98 (1993) 5648.

[36] J.P. Perdew, K. Burke, M. Ernzerhof, Generalized gradient approximation made simple [Phys. Rev. Lett. 77, 3865 (1996)], Phys. Rev. Lett. 78 (1997), https://doi.org/10.1103/PhysRevLett.78.1396, 1396–1396.

[37] C. Adamo, V. Barone, Toward reliable density functional methods without adjustable parameters: the pbe0 model, J. Chem. Phys. 110 (13) (1999) 6158–6170, https://doi.org/10.1063/1.478522.

[38] J. Heyd, G.E. Scuseria, M. Ernzerhof, Erratum: "Hybrid functionals based on a screened coulomb potential" [J. Chem. Phys.118, 8207 (2003)], J. Chem. Phys. 124 (21) (2006), https://doi.org/10.1063/1.2204597.

[39] J. Heyd, G.E. Scuseria, Assessment and validation of a screened coulomb hybrid density functional, J. Chem. Phys. 120 (16) (2004) 7274–7280, https://doi.org/10.1063/1.1668634.

[40] J. Heyd, J.E. Peralta, G.E. Scuseria, R.L. Martin, Energy band gaps and lattice parameters evaluated with the heyd-scuseria-ernzerhof screened hybrid functional, J. Chem. Phys. 123(17).https://doi.org/10.1063/1.2085170.

[41] J. Heyd, G.E. Scuseria, M. Ernzerhof, Hybrid functionals based on a screened coulomb potential, J. Chem. Phys. 118 (18) (2003) 8207–8215, https://doi.org/10.1063/1.1564060.

[42] O.A. Vydrov, G.E. Scuseria, J.P. Perdew, Tests of functionals for systems with fractional electron number, J. Chem. Phys. 126 (15).https://doi.org/10.1063/1.2723119.

[43] O.A. Vydrov, J. Heyd, A.V. Krukau, G.E. Scuseria, Importance of short-range versus long-range hartree-fock exchange for the performance of hybrid density functionals, J. Chem. Phys. 125(7).https://doi.org/10.1063/1.2244560.

[44] D. Cho, K.C. Ko, Y. Ikabata, K. Wakayama, T. Yoshikawa, H. Nakai, J.Y. Lee, Effect of hartree-fock exact exchange on intramolecular magnetic coupling constants of organic diradicals, J. Chem. Phys. 142 (2) (2015), https://doi.org/10.1063/1.4905561 024318.

[45] S. Shil, C. Herrmann, Performance of range-separated hybrid exchange correlation functionals for the calculation of magnetic exchange coupling constants of organic diradicals, J. Comp. Chem. 39 (13) (2018) 780–787, https://doi.org/10.1002/jcc.25153.

[46] M.G. Medvedev, I.S. Bushmarinov, J. Sun, J.P. Perdew, K.A. Lyssenko, Density functional theory is straying from the path toward the exact functional, Science 355 (6320) (2017) 49–52, https://doi.org/10.1126/science.aah5975.

[47] W. Heisenberg, Zur theorie des ferromagnetismus, Zeitschrift fnür Physik 49 (9–10) (1928) 619–636, https://doi.org/10.1007/BF01328601.

[48] L. Noodleman, Valence bond description of antiferromagnetic coupling in transition metal dimers, J. Chem. Phys. 74 (10) (1981) 5737–5743, https://doi.org/10.1063/1.440939.

[49] E. Ruiz, J. Cano, S. Alvarez, P. Alemany, Broken symmetry approach to calculation of exchange coupling constants for homobinuclear and heterobinuclear transition metal complexes, J. Comput. Chem. 20 (13) (1999) 1391–1400, https://doi.org/10.1002/(SICI)1096-987X(199910)20:13<1391::AID-JCC6>3.0.CO;2-J.

[50] J.J. Phillips, J.E. Peralta, Towards the blackbox computation of magnetic exchange coupling parameters in polynuclear transition-metal complexes: Theory, implementation, and application, J. Chem. Phys. 138 (17) (2013), https://doi.org/10.1063/1.4802776.

[51] R.P. Joshi, J.J. Phillips, J.E. Peralta, Magnetic exchange couplings in heterodinuclear complexes based on differential local spin rotations, J. Chem. Theory Comput. 12 (4) (2016) 1728–1734, https://doi.org/10.1021/acs.jctc.6b00112.

[52] M.J. Han, T. Ozaki, J. Yu, Electronic structure, magnetic interactions, and the role of ligands in $Mn_n(n = 4, 12)$ single-molecule magnets, Phys. Rev. B 70 (2004), https://doi.org/10.1103/PhysRevB.70.184421 184421.

[53] T. Steenbock, J. Tasche, A.I. Lichtenstein, C. Herrmann, A green's-function approach to exchange spin coupling as a new tool for quantum chemistry, J. Chem. Theory Comput. 11 (12) (2015) 5651–5664, https://doi.org/10.1021/acs.jctc.5b00349, pMID: 26579585.

[54] M.J. Frisch, G.W. Trucks, H.B. Schlegel, G.E. Scuseria, M.A. Robb, J.R. Cheeseman, G. Scalmani, V. Barone, G.A. Petersson, H. Nakatsuji, X. Li, M. Caricato, A.V. Marenich, J. Bloino, B.G. Janesko, R. Gomperts, B. Mennucci, H.P. Hratchian, J.V. Ortiz, A.F. Izmaylov, J.L. Sonnenberg, D. Williams-Young, F. Ding, F. Lipparini, F. Egidi, J. Goings, B. Peng, A. Petrone, T. Henderson, D. Ranasinghe, V.G. Zakrzewski, J. Gao, N. Rega, G. Zheng, W. Liang, M. Hada, M. Ehara, K. Toyota, R. Fukuda, J. Hasegawa, M. Ishida, T. Nakajima, Y. Honda, O. Kitao, H. Nakai, T. Vreven, K. Throssell, J.A. Montgomery Jr, J.E. Peralta, F. Ogliaro, M.J. Bearpark, J.J. Heyd, E.N. Brothers, K.N. Kudin, V.N. Staroverov, T.A. Keith, R. Kobayashi, J. Normand, K. Raghavachari, A.P. Rendell, J.C. Burant, S.S. Iyengar, J. Tomasi, M. Cossi, J.M. Millam, M. Klene, C. Adamo, R. Cammi, J.W. Ochterski, R. L. Martin, K. Morokuma, O. Farkas, J.B. Foresman, D.J. Fox, Gaussian 16 Revision C.01, Gaussian Inc., Wallingford CT, 2016.

[55] C. Lee, W. Yang, R.G. Parr, Development of the colle-salvetti correlation-energy formula into a functional of the electron density, Phys. Rev. B 37 (1988) 785.

[56] P.J. Stephens, F.J. Devlin, C.F. Chabalowski, M.J. Frisch, Ab initio calculation of vibrational absorption and circular dichroism spectra using density functional force fields, J. Phys. Chem. 98 (1994) 11623.

[57] R.H. Hertwig, W. Koch, On the parameterization of the local correlation functional. what is Becke-3-LYP?, Chem. Phys. Lett. 268 (5) (1997) 345–351, https://doi.org/10.1016/S0009-2614(97)00207-8.

[58] O.A. Vydrov, G.E. Scuseria, Assessment of a long-range corrected hybrid functional, J. Chem. Phys. 125(23).https://doi.org/10.1063/1.2409292.

[59] J.A. Montgomery, M.J. Frisch, J.W. Ochterski, G.A. Petersson, A complete basis set model chemistry. VII. Use of the minimum population localization method, J. Chem. Phys. 112 (15) (2000) 6532–6542, https://doi.org/10.1063/1.481224.

[60] Y.Y. Masamichi Nishino, Syusuke Yamanaka, K. Yamaguchi, Theoretical approaches to direct exchange couplings between divalent chromium ions in naked dimers, tetramers, and clusters, J. Phys. Chem. A 101 (4) (1997) 705–712, https://doi.org/10.1021/jp962091l.

[61] T. Onishi, D. Yamaki, K. Yamaguchi, Y. Takano, Theoretical calculations of effective exchange integrals by spin projected and unprojected broken-symmetry methods. I. Cluster models of K2NiF4-type solids, J. Chem. Phys. 118 (21) (2003) 9747–9761, https://doi.org/10.1063/1.1567251.

[62] G. De Munno, T. Poerio, G. Viau, M. Julve, F. Lloret, Ferromagnetic coupling in the bis(-end-on-azido)iron(III) dinuclear complex anion of [$Fe^{II}(bpym)_3$]$_2$[Fe(N$_3$)$_{10}$]$^-$+2H$_2$O, Angen, Chmi. Int. Ed. Eng. 36 (13–14) (1997) 1459–1461, https://doi.org/10.1002/anie.199714591, arXiv: https://onlinelibrary.wiley.com/doi/pdf/10.1002/anie.199714591.

[63] S. Naiya, M.G.B. Drew, C. Diaz, J. Ribas, A. Ghosh, Synthesis crystal structure, and magnetic properties of a very rare double -1,1-azido- and a -1,1-(ome)-bridged Fe^{III} dimer containing a n, n, o-donor tridentate schiff base ligand, Eur. J. Inorg. Chem. 2011 (32) (2011) 4993–4999, https://doi.org/10.1002/ejic.201100552, arXiv: https://onlinelibrary.wiley.com/doi/pdf/10.1002/ejic.201100552.

[64] K.R. Reddy, M.V. Rajasekharan, J.-P. Tuchagues, Synthesis, structure, and magnetic properties of Nn(salpn)N$_3$, a helical polymer, and Fe(salpn)N$_3$, a ferromagnetically coupled dimer (salpnh2 = n, n-bis(salicylidene)-1,3-diaminopropane), Inorg. Chem. 37 (23) (1998) 5978–5982, https://doi.org/10.1021/ic971592y.

[65] H. Adams, N.A. Bailey, J.D. Crane, D.E. Fenton, J.-M. Latour, J.M. Williams, Manganese(ii) and iron(III) complexes of the tridentate ligands bis (benzimidazol-2-ylmethyl)-amine (l1) and -methylamine (l2). crystal structures of [Mn$_{l1}$(CH$_3$CO$_2$)2], [Fe$_{l2}$Cl$_3$], and [Fe2l12(–O)–(CH$_3$)3CCO22] [Clo$_4$]2, J. Chem. Soc., Dalton Trans. (1990) 1727–1735.

[66] R.E. Norman, R.C. Holz, S. Menage, L. Que, J.H. Zhang, C.J. O'Connor, Structures and properties of dibridged (μ-oxo)diiron(iii) complexes. effects of the Fe-O-Fe angle, Inorg. Chem. 29 (23) (1990) 4629–4637, https://doi.org/10.1021/ic00348a010.

[67] J.W. Shin, S.R. Rowthu, J.E. Lee, H.I. Lee, K.S. Min, Syntheses, structures and magnetic properties of dinuclear oxo-bridged iron(III) complexes, Polyhedron 33 (1) (2012) 25–32, https://doi.org/10.1016/j.poly.2011.11.018.

[68] J.B. Vincent, J.C. Huffman, G. Christou, Q. Li, M.A. Nanny, D.N. Hendrickson, R.H. Fong, R.H. Fish, Modeling the dinuclear sites of iron biomolecules: synthesis and properties of Fe$_2$O(OAc)$_2$Cl$_2$(bipy)$_2$ and its use as an alkane activation catalyst, J. Am. Chem. Soc. 110 (20) (1988) 6898–6900, https://doi.org/10.1021/ja00228a057.

[69] E.-Q. Gao, L.-H. Yin, J.-K. Tang, P. Cheng, D.-Z. Liao, Z.-H. Jiang, S.-P. Yan, Synthesis, crystal structure and magnetic properties of a new dialkoxo-bridged diiron(III) complex, Polyhedron 20 (7) (2001) 669–673, https://doi.org/10.1016/S0277-5387(01)00731-8.

[70] Y. Yahsi, H. Kara, L. Sorace, O. Buyukgungor, Mono- and dinuclear Fe(III) complexes with the N$_2$O$_2$ donor 5-chlorosalicylideneimine ligands; synthesis, x-ray structural characterization and magnetic properties, Inorganica Chim. Acta 366 (1) (2011) 191–197, https://doi.org/10.1016/j.ica.2010.10.027.

[71] F. Banse, V. Balland, C. Philouze, E. Rivire, L. Tchertanova, J.-J. Girerd, Mono- and dinuclear feiii complexes with the tridentate n-ethyl-n-(2-aminoethyl) salicylaldiminato ligand. X-ray structures, magnetic and spectroscopic properties, Inorganica Chim. Acta 353 (2003) 223–230, https://doi.org/10.1016/S0020-1693(03)00292-5.

[72] S.J. Barclay, P.E. Riley, K.N. Raymond, Coordination chemistry of microbial iron transport compounds. 26. dimeric dialkoxo-bridged iron(III) complexes of linear dihydroxamate ligands, Inorg. Chem. 23 (14) (1984) 2005–2010, https://doi.org/10.1021/ic00182a006.

[73] J. Cabrero, C.J. Calzado, D. Maynau, R. Caballol, J.P. Malrieu, Metal-ligand delocalization in magnetic orbitals of binuclear complexes, J. Phys. Chem. A 106 (35) (2002) 8146–8155, https://doi.org/10.1021/jp0204410.

[74] R.P. Joshi, K. Trepte, K.P.K. Withanage, K. Sharkas, Y. Yamamoto, L. Basurto, R.R. Zope, T. Baruah, K.A. Jackson, J.E. Peralta, Fermi-Löwdin orbital self-interaction correction to magnetic exchange couplings, J. Chem. Phys. 149 (2018), https://doi.org/10.1063/1.5050809 164101.